Local magnetic field distributions. II. Further results

T. C. Choy
Department of Physics and Astronomy, Michigan State University, East Lansing, Michigan 48824
and Physics Department, Imperial College of Science and Technology, London SW7 2BZ, United Kingdom

David Sherrington
Physics Department, Imperial College of Science and Technology, London SW7 2BZ, United Kingdom

M. Thomsen* and M. F. Thorpe
Department of Physics and Astronomy, Michigan State University, East Lansing, Michigan 48824
(Received 13 November 1984)

The concept and character of the local magnetic field distribution $P(h)$, developed in an earlier paper, is extended to higher space and spin dimensions and to several special but spatially periodic systems, disorder being the subject of a future paper. For Ising spins on standard lattices, $P(h)$ is shown to have a shape which is dimension dependent but relatively coordination independent. While in two dimensions (2D) $P(h)$ has a dip at $h=0$ at T_c, in 3D it is extremely flat near the origin, in 4D it is pseudo-Gaussian, while in all dimensions it is qualitatively similar to a discrete form of the corresponding universal block-spin probability function. Bethe lattices, studied for all spin dimensions, are shown to be quite different. Results are also presented for $P(h)$ and the ground-state degeneracies of some one-dimensional frustrated systems exhibiting high-degeneracy disorder points.

I. INTRODUCTION

This paper is the second in a series of three concerned with the local magnetic field distribution $P(\mathbf{h},T)$ in classical spin systems. The first,[1] referred to hereafter as paper I, was concerned explicitly with Ising systems, both with the formal information contained in $P(h,T)$ and with the evaluation of $P(h,T)$ in some soluble one-dimensional (1D) and 2D cases. This paper extends the study to other systems without spatial disorder. The case of spatial disorder of the Hamiltonian is the subject of the third paper[2] in the series (paper III).

Section II of this paper is concerned with further evaluations of $P(h,T)$ for Ising models on higher-dimensional conventional lattices and on Bethe lattices. Since the higher-dimensional standard lattices have not yielded to exact solution they are studied by Monte Carlo simulation. The Bethe lattice is exactly soluble. Just as $P(h,T)$ was found in paper I to have a qualitatively similar shape for all two-dimensional lattices close to criticality, also a qualitative universality is found in the shape of $P(h,T)$ in 3D. However, the shape at T_c is very different in these higher dimensions. In 2D, $P(h,T_c)$ has a dip at $h=0$. By contrast, in 3D, $P(h,T_c)$ is very flat around the origin, while for 4D, $P(h,T_c)$ is still very much like its quasi-Gaussian high-temperature form. These shapes are qualitatively analogous[3,4] to those of the corresponding block-spin distribution functions in the limit $\xi \gg L \gg a$, where ξ is the correlation length, L is the block dimension, and a is the lattice scale.

Section III considers some simple but interesting one-dimensional examples of systems with finite residual entropies at zero temperature. These are studied as background to more complicated models with frustration[5–7] and systems with disorder [as studied further in paper III (Ref. 2)].

In Sec. IV the formulation of statistical mechanics in terms of $P(\mathbf{h},T)$ is extended to vector spins. Explicit exact evaluations of $P(\mathbf{h},T)$ are presented for Bethe lattices.

II. ISING MODELS

A natural extension of previous studies[1] is to examine the structure of $P(h)$ for higher-dimensional lattices to gauge the effect of dimensionality.[8] Unfortunately, no exact solutions are known for Ising models on standard finite-dimensional lattices of dimension greater than two. Consequently, we must turn to approximate methods or to artificial lattices, such as the Bethe lattice. We consider these in turn.

Frank *et al.*[9] developed an approximation procedure which effectively allowed them to estimate the moments of $P(h)$ for a variety of three-dimensional lattices at T_c. In principle, one can recover the distribution from the moments, but in practice the errors are too large, so that negative weights appear in the reconstructed distribution.

Since it appeared that little progress could be made analytically on standard lattices, Monte Carlo simulations were performed. In all cases these were for nearest-neighbor Ising models characterized by the Hamiltonian

$$\mathcal{H}=-\frac{1}{2}\sum_{i,j}J_{ij}\sigma_i\sigma_j\ ,\quad J_{ij}=\begin{cases}J & \text{for nearest neighbors}\\ 0 & \text{otherwise}\ ,\end{cases}$$

$$\sigma_i=\pm 1\ . \tag{1}$$

A variety of lattices and temperatures were studied. The temperature scale for these simulations was set by the

values for T_c based on high-temperature series and reported elsewhere: $k_B T_c/J = 2.7044 \pm 0.0001$ (diamond),[10] 4.5108 ± 0.0002 (simple cubic),[10] 6.3533 ± 0.0010 (body-centered cubic),[10] 9.7952 ± 0.0005 (face-centered cubic),[10] and $k_B T_c/J = 6.6817 \pm 0.0015$ (four-dimensional simple hypercubic).[11] No attempt was made to locate T_c precisely in these simulations since detailed information (such as critical exponents) was not sought.

Simulations generally have the most trouble converging when $T = T_c$. However, since it is known that $P(h)$, defined by

$$P(h) = N^{-1} \sum_i \left\langle \delta \left[h - \sum_j J_{ij} \sigma_j \right] \right\rangle \tag{2}$$

is symmetric at T_c, only $P_s(h) = \frac{1}{2}[P(h) + P(-h)]$ need be extracted at the critical temperature. This function couples to the energy, or equivalently to the nearest-neighbor correlation $\langle \sigma_0 \sigma_1 \rangle$, which is less sensitive to critical fluctuations than are the magnetization and $P_a(h) = \frac{1}{2}[P(h) - P(-h)]$. The criterion for convergence at T_c was thus taken to be that $\langle \sigma_0 \sigma_1 \rangle$ should equilibrate. This correlation can then be compared with estimates obtained from high-temperature series.

The numerical simulations were performed on lattices of varying sizes and with periodic boundary conditions, employing the standard Metropolis algorithm.[12] Technical details associated with these simulations can be found in Ref. 8. Briefly, however, a given system would initially be brought into equilibrium and then be allowed to remain there while data was accumulated for thermal averages. Statistical errors quoted refer to the fluctuations in the thermal average during the second half of the averaging part of the simulation. The simulation was performed on three different lattice sizes (four at T_c), with the largest system containing roughly 30 000 spins. Then the data was plotted against the inverse of the number of spins in the system to allow extrapolation to infinite size.

The results of these extrapolations can now be compared to high-temperature series results[10,11] to gauge the accuracy of the simulation. This comparison for $\langle \sigma_0 \sigma_1 \rangle_{T_c}$ (see Table I), shows reasonable agreement between the two sets of results. Based on this, one would expect the data to be accurate to within a few (3 or 4) percent, which is sufficient to determine the general nature of $P(h)$.

Figure 1 displays $P(h)$ for four different three-dimensional lattices. All of these lattices show an extremely flat profile near T_c. Whether there is a slight dip or bump at $h = 0$ cannot be conclusively determined from this data, but it is clear that these profiles differ from those of the two-dimensional lattices which exhibit a clear zero-field minimum at T_c. It is also evident that in three dimensions, as in two, coordination number plays very little role in the qualitative profile.

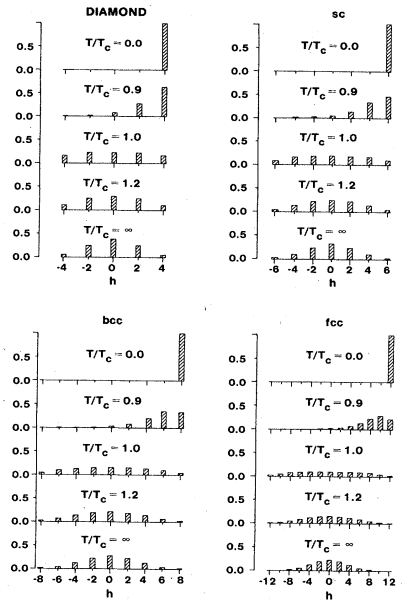

FIG. 1. $P(h,T)$ for four different three-dimensional Ising ferromagnets.

To see the dimensional dependence explicitly, it is constructive to look at the simple cubics in dimensions one through four (i.e., the linear chain, the square net, the simple cubic, and the four-dimensional simple hypercubic). These lattices all have coordination number equal to twice their dimension. The infinite-dimension limit yields the mean-field result, to be discussed later, and will be included with this group too. These lattices have critical temperatures scaling roughly with coordination z, providing a consistent way to normalize all the temperatures at which $P(h)$ was measured (either analytically or by simulation). More exactly, one finds $0 \leq T_c/z \leq 1$, where the lower limit corresponds to the linear chain and the upper limit to mean-field theory.

The graphs in Fig. 2 show $P(h)$ for each of the five systems measured at each of the five (renormalized) transition temperatures. The profiles for any group of lattices above their transition temperatures are very similar provided that they are measured at the same renormalized temperature. The most dramatic example of this is seen by looking at the one-, two-, and three-dimensional data at a temperature corresponding to T_c in three dimensions; all three profiles are extremely flat.

Below T_c the symmetry is broken and the profiles lose much of their similarity. In the case of the four-dimensional hypercubic the approach to mean-field theory can be seen by noting the development of a peak away from $h = 0$, rapidly approaching $h = Jz$, the zero-temperature result, as the temperature is lowered.

Clearly, the coordination of a lattice affects $P(h)$ in

TABLE I. Nearest-neighbor spin-spin correlation function at the critical point $\langle \sigma_0 \sigma_1 \rangle_{T_c}$ as obtained from Monte Carlo simulations and compared to high-temperature series results.

Lattice	High-T series	Simulation
Diamond	0.437 ±0.003	0.44±0.01
sc	0.3307±0.0001	0.34±0.01
bcc	0.2732±0.0002	0.28±0.01
fcc	0.2474±0.0001	0.26±0.01
4D simple hypercubic	0.188 ±0.003	0.20±0.01

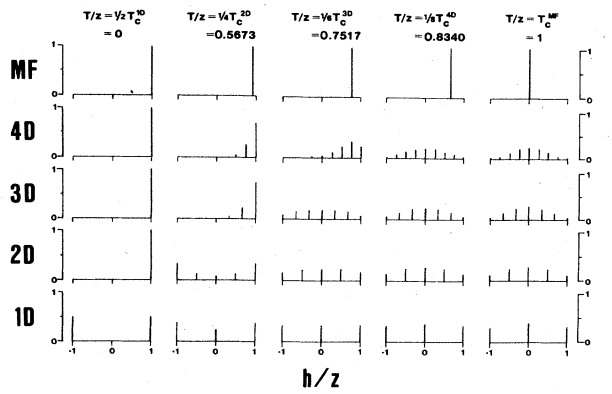

FIG. 2. $P(h,T)$ for simple (hyper) cubics of dimensions one through four and for the mean-field limit.

that it determines the number of δ functions. Additionally, it helps set the temperature scale. Beyond that, however, the profile of $P(h)$ is more sensitive to the dimension. At T_c this dimension dependence comes primarily from the two-spin correlations $\langle\sigma_0\sigma_1\rangle$, reflecting the amount of short-range order which precedes the onset of long-range order. This does not imply, however, that higher-order spin correlations are insignificant. They determine the higher-order moments of $P(h)$ and their neglect or incorrect determination results in the violation of sum rules and inequalities, giving rise, for example, to unphysical negative weights in the distribution.[6] Another useful measure is provided by the parameter

$$v=[\overline{h^2}-(\overline{h})^2]/z \tag{3}$$

introduced in paper I. Table II gives values for this parameter for the various three-dimensional lattices studied at $T=T_c$. They are substantially less than the corresponding values found for two-dimensional lattices,[1] indicating that less local order is present at the onset of long-range order in three dimensions than in two dimensions. A further illustration is given in Figs. 3 and 4 which show snapshots of the two- and three-dimensional hypercubes at $T\simeq T_c$ and demonstrate clearly the presence of larger domains in the two-dimensional case.

We now introduce a general formula for $P(h)$ which is useful for identifying the contributions from various correlations and which simplifies significantly on lattices with no closed loops; it also admits straightforward generalization to classical vector spins, discussed later.

We start with the definition[1] of Eq. (1) in paper I:

$$P_i(h)=\mathrm{Tr}[e^{-\beta\mathscr{H}}\delta(h-h_i)]/\mathrm{Tr}e^{-\beta\mathscr{H}},\quad h_i=\sum_j J_{ij}\sigma_j\ . \tag{4}$$

This can be rearranged to give

$$\begin{aligned}P_i(h)&=\mathrm{Tr}'\mathrm{Tr}_i[e^{-\beta\mathscr{H}}\delta(h-h_i)]/\mathrm{Tr}e^{-\beta\mathscr{H}}\\&=\mathrm{Tr}'[e^{-\beta\mathscr{H}'}Z_1(\beta h_i)\delta(h-h_i)]/\mathrm{Tr}e^{-\beta\mathscr{H}}\ ,\end{aligned} \tag{5}$$

where $\mathscr{H}'=\mathscr{H}+h_i\sigma_i$ is independent of σ_i, Tr_i is the trace over σ_i while Tr' denotes the trace over all other spins, and $Z_1(\beta h_i)$ is the partition function of a single free spin in a field h_i. Taking advantage of the δ function, we obtain

TABLE II. Local-field fluctuations v at T_c for 3D lattices.

Lattice	v
Diamond	0.88
sc	1.01
bcc	1.12
fcc	1.57

$$P_i(h)=\langle\delta(h-h_i)\rangle' Z_1(\beta h)\frac{\mathrm{Tr}'e^{-\beta\mathscr{H}'}}{\mathrm{Tr}e^{-\beta\mathscr{H}}}\ , \tag{6}$$

where the notation $\langle\ \rangle'$ refers to a thermal average using the Hamiltonian $\mathscr{H}'$. $\langle\delta(h-h_i)\rangle'$ involves only spin correlations not containing σ_i. On standard lattices its evaluation is still a formidable undertaking requiring knowledge of multispin correlations.[6] On the other hand, for special lattices with no closed loops, such as the Bethe lattice, Eq. (6) can be exploited to advantage. Passage to mean-field theory and m-vector generalizations follow readily.

Because of its large surface area, calculations on a Bethe lattice must be approached with caution. For instance, Eggarter[13] pointed out that for free boundaries the Bethe lattice has no phase transition. However, the more traditional Bethe[14]-Peierls[15] approach,[16] which assumes boundary conditions determined self-consistently, does have a phase transition. This latter approach will be used in our discussion.

The Bethe-Peierls method,[16,17] leading to the self-consistent field equation (4) below, has been shown to be an exact solution on a Bethe lattice with the appropriate boundary condition, as discussed above, although it is only approximate for conventional lattices. An effective Hamiltonian is assumed for a cluster consisting of site 0 and its z nearest neighbors:

$$\mathscr{H}_z=-J\sum_{j=1}^{z}\sigma_0\sigma_j-H_0\sigma_0-H_1\sum_{j=1}^{z}\sigma_j\ . \tag{7}$$

H_0 is an external field included for the purpose of obtaining the self-consistency equation

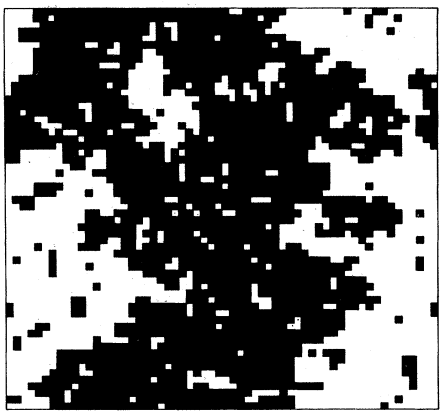

FIG. 3. Snapshot of 60×60 2D Ising lattice at $T/T_c=1.01$ after 11 500 Monte Carlo steps per spin. Black area denotes up-spins, white area denotes down-spins.

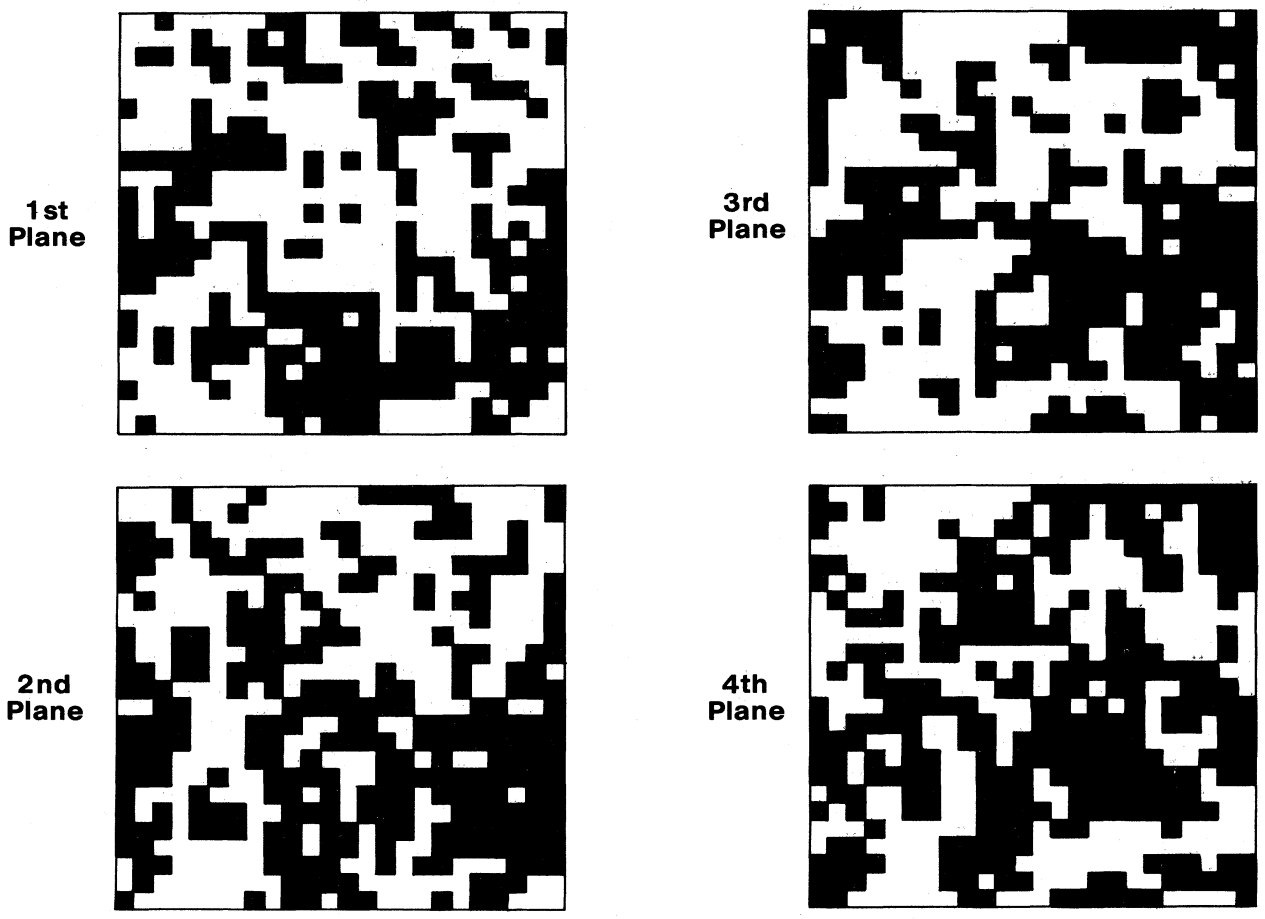

FIG. 4. Snapshots of $24\times24\times24$ 3D Ising lattice at $T/T_c=1.01$ after 4800 Monte Carlo steps. The pictures indicate four adjacent planes.

$$\langle\sigma_0\rangle=\langle\sigma_j\rangle\ , \tag{8}$$

via

$$\frac{\partial}{\partial(\beta H_0)}\ln Z=\frac{\partial}{\partial(\beta H_1)}\ln Z\ , \tag{9}$$

where

$$Z=e^{\beta H_0}\{2\cosh[\beta(J+H_1)]\}^z + e^{-\beta H_0}\{2\cosh[\beta(J-H_1)]\}^z \tag{10}$$

is the partition function associated with Eq. (7). H_0 may then be set equal to 0. H_1 is an effective, temperature-dependent field acting on the σ_j's accounting for both H_0 and interactions with all the $(z-1)$ remaining neighbors (other than σ_0) of each σ_j. Straightforward algebra yields [from Eq. (9)]

$$\frac{\tanh[\beta H_1/(z-1)]}{\tanh(\beta H_1)}=\tanh(\beta J) \tag{11}$$

and the critical temperature

$$\tanh(\beta_c J)=1/(z-1),\quad \beta_c=1/k_B T_c\ . \tag{12}$$

Equation (11) can be rewritten as

$$(1-t)Y^{z-1}-2t\sum_{i=1}^{z-2}Y^i+(1-t)=0\ , \tag{13}$$

where $Y=\lambda_1^{1/z-1}$, $\lambda_1=e^{-2\beta H_1}$, and $t=\tanh(\beta J)$; a form suitable for analytic solution for H_1 up to $z=10$.

We quote some of the results below in terms of $x=e^{-2\beta J}$.

For $z=3$,

$$\lambda_1=\tfrac{1}{2}[x^{-2}-2x^{-1}-1+(x^{-2}-x^{-1})(1-2x-3x^2)^{1/2}]\ . \tag{14}$$

For $z=4$,

$$\lambda_1=\tfrac{1}{2}[x^{-3}-3x^{-1}+(x^{-2}-1)(x^{-2}-4)^{1/2}]\ . \tag{15}$$

For $z=5$,

$$\lambda_1=\{[c+(c^2-4)^{1/2}]/2\}^4\ , \quad \text{where} \quad c=[1-x+(5x^2+2x+1)^{1/2}]/2x\ . \tag{16}$$

For $z=6$,

$$\lambda_1=\{[D+(D^2-4)^{1/2}]/2\}^5 ,$$

where (17)

$$D=[x^{-1}+(x^{-2}+4)^{1/2}]/2 .$$

With these fundamental equations in place we now return to Eq. (6) for the evaluation of $P(h)$ for Bethe lattices. Because there are no closed loops the $\mathrm{Tr}' e^{-\beta\mathcal{H}'}$ term splits up into contributions from z independent lattices

$$\mathrm{Tr}' e^{-\beta\mathcal{H}'}=(\mathrm{Tr}_j e^{\beta H_1\sigma_j})^z=(2\cosh\beta H_1)^z \tag{18}$$

while

$$\mathrm{Tr}' e^{-\beta\mathcal{H}'}\delta\left[h-J\sum_j\sigma_j\right]=\int\frac{dx}{2\pi}e^{-ihx}(\mathrm{Tr}_j e^{(\beta H_1+iJx)\sigma_j})^z=\int\frac{dx}{2\pi}e^{-ihx}[2\cosh(\beta H_1+iJx)]^z$$

$$=\sum_{s=-z}^{z}C^z_{(z+s)/2}e^{\beta H_1 s}\delta(h-Js) . \tag{19}$$

Thus,

$$P(h)=\frac{e^{\beta h H_1/J}}{Z_0}(2\cosh\beta h)\sum_{s=-z}^{z}C^z_{(z+s)/2}\delta(h-Js) , \tag{20}$$

where

$$Z_0=\{2\cosh[\beta(J+H_1)]\}^z+\{2\cosh[\beta(J-H_1)]\}^z \tag{21}$$

with H_1 given as above, zero above T_c, finite below.

An alternative to the use of Eq. (6) is to note that the moments of $(h/J)=\sum_j\sigma_j$ follow directly from Eq. (7),

$$\langle(h/J)^n\rangle=Z_0^{-1}[\partial/\partial(\beta H_1)]^n Z_0 \tag{22}$$

and further that, given all the moments up to $\langle(h/J)^z\rangle$, one can in principle solve for the weights w_s in the $(2z+1)$ delta functions constituting $P(h)$. In practice, however, the procedure is tedious and complicated.[18]

The passage to mean-field theory follows from Eqs. (20) or (22) by taking $z\to\infty$ keeping Jz constant, while H_1 should scale with Jz. Then,

$$Z_0=[2\cosh(\beta H_1)]^z \tag{23}$$

and

$$H_1/Jz=\tanh(\beta H_1) , \tag{24}$$

so that

$$\beta_c=zJ . \tag{25}$$

Equation (22) also shows that

$$\langle(h/J)^n\rangle=z(z-1)\cdots(z-n-1)\tanh^n(\beta H_1)+O(z^{n-1}) \tag{26}$$

or

$$\langle(h/Jz)^n\rangle=\tanh^n(\beta H_1)+O(1/z) , \tag{27}$$

i.e.,

$$P(h)=\delta(h-Jz\tanh(\beta H_1))=\delta(h-H_1) , \tag{28}$$

from Eq. (24), which is another way of saying that mean-field theory becomes exact when $z\to\infty$ with H_1 defining precisely the local field.[19]

As demonstrated in paper I, Eq. (52), for $z=3$ the weights w_s can be expressed in terms of the magnetization m, per spin, and $\epsilon=\langle\sigma_0\sigma_1\rangle$:

$$w_{\pm1}=\frac{1}{2}\left[\frac{3[\tanh(3\beta J)-\epsilon]}{3\tanh(3\beta J)-\tanh(\beta J)}\pm\frac{3m[\tanh(3\beta J)-1]}{\tanh(3\beta J)-3\tanh(\beta J)}\right] ,$$

$$w_{\pm3}=\frac{1}{2}\left[\frac{3\epsilon-\tanh(\beta J)}{3\tanh(3\beta J)-\tanh(\beta J)}\pm\frac{m[1-3\tanh(\beta J)]}{\tanh(3\beta J)-3\tanh(\beta J)}\right] . \tag{29}$$

For the Bethe lattice with $z=3$,

$$m=\langle\sigma_0\rangle=\frac{1-\lambda_1^2}{1+\lambda_1^2+2\lambda_1 x} \tag{30}$$

and

$$\epsilon=\langle\sigma_0\sigma_1\rangle=\frac{1+\lambda_1^2-2\lambda_1 x}{1+\lambda_1^2+2\lambda_1 x} . \tag{31}$$

In Fig. 5, $P(h)$ is plotted against h/z for $z=3$, 4, 6, and infinity. It is symmetric for $T\geq T_c$, reflecting the fact that the magnetization is zero. At infinite temperature, the weights are determined by counting the number of ways to make a particular value of h.[1] Since there are more ways to make $h=0$, the distribution is peaked there. When $T=T_c$, the distribution is still peaked at small h, with more weight being at $h=0$ as the mean-field limit is approached. The symmetry is broken below T_c when spontaneous magnetization sets in. Again the approach to mean-field theory is seen as the maximum in $P(h)$ moves from $h=Jz$, with $z=3$, to $h=Jzm$ for larger z.

It is apparent that there is a strong dependence of $P(h)$ on the coordination number z for Bethe lattices. Not only is the number of delta functions clearly determined by z, but also the profile of the distribution, particularly at T_c, is sensitive to z. As argued previously this arises from the strong dependence on z of the two-spin correlation,

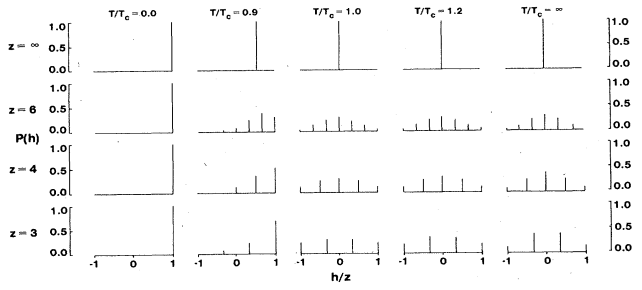

FIG. 5. $P(h,T)$ for Ising spins on Bethe lattices of coordination 3, 4, 6, and ∞.

$$\langle \sigma_0 \sigma_1 \rangle_{T_c} = (z-1)^{-1} , \tag{32}$$

the only spin correlation of significance on the Bethe lattice.

To conclude our studies of Ising systems on regular lattices we return to the question of universality or quasiuniversality in the shape of $P(h)$ observed in paper I and this paper. As we have already remarked we find a qualitatively dimension-dependent but relatively coordination-number-independent quasiuniversality in the shape of $P(h)$ at $T \sim T_c$; in particular, we find a flattening at the origin for $d=3$ and a dip for $d=2$. These behaviors are reminiscent of those obtained by other authors[3,4] (from renormalization-group analysis[3] or finite-size scaling studies of Monte Carlo simulations[4]) for the block-spin distribution $P_L(S)$, defined below, where L is the block scale and S is the normalized block spin in the range $\xi \gg L \gg a$, where ξ is the correlation length and a is the lattice spacing. Within this range, the block-spin distribution, now called $P_\infty(S)$, is believed to be universal[3,20] and non-Gaussian for $d < d_c$, the upper critical dimension. The results found[3,4] for $P_\infty(S)$ for $d=3$ and $d=2$ are qualitatively very similar to those we find for the local $P(h)$, albeit that $P_\infty(S)$ is a continuous function and $P(h)$ is a discrete one. [Figures 7(a) and 7(b) show this comparison, and also with another distribution defined below.]

The block-distribution function $P(S)$ is defined by

$$P_L(S) = \left\langle \delta \left[S - n_L^{-1} \sum_{j \in \Omega_L} S_j \right] \right\rangle , \tag{33}$$

where Ω_L denotes a block of linear dimension L and n_L is the number of spins within Ω_L. We shall not consider this quantity for general L but note that from $P(h)$ we can readily calculate the block-spin distribution for the block consisting of a central spin and its z nearest neighbors; we denote this $P^{z+1}(S)$. For notational brevity it is convenient to work with the related quantity $\tilde{P}^{z+1}(t)$ given by[21]

$$\tilde{P}^{z+1}(t) = \left\langle \delta \left[t - \sum_{j=0}^{z} S_j \right] \right\rangle , \tag{34}$$

$$P^{z+1}(S) = (z+1) \tilde{P}^{z+1}[(z+1)^{-1} S] . \tag{35}$$

For convenience we set the nearest-neighbor exchange J equal to 1. Then, we find

$$\tilde{P}^{z+1}(t) = \langle \delta(t - S_0 - h_i) \rangle = \int dh \, \langle \delta(h - h_i) \delta(h - t + S_0) \rangle . \tag{36}$$

$$\langle \delta(h-h_i)\delta(h-t+S_0) \rangle = \frac{\mathrm{Tr}[e^{-\beta H} \delta(h-h_i)] \mathrm{Tr}[e^{+\beta h S_0} \delta(h-t+S_0)]}{Z \, \mathrm{Tr}(e^{-\beta h S_0})} = \frac{e^{\beta h} P(h) \delta(h-t+1) + e^{-\beta h} P(h) \delta(h-t-1)}{e^{\beta h} + e^{\beta h}} . \tag{37}$$

Thus,

$$\tilde{P}^{z+1}(t) = \left[\frac{e^{\beta h} P(h)}{e^{\beta h} + e^{-\beta h}} \right]_{h=t-1} + \left[\frac{e^{-\beta h} P(h)}{e^{\beta h} + e^{-\beta h}} \right]_{h=t+1} . \tag{38}$$

In Fig. 6 we plot $\tilde{P}^{z+1}(t)$ for the square net at T_c using our results from paper I; $P^{z+1}(S)$ follows by simple scaling. Note that it has one extra δ function compared with $P(h)$, a first step on the route to the quasicontinuous $P_L(S)$ as $L \to \infty$. Equation (38) can be understood physically since $P_\pm(h) = e^{\pm \beta h}/(2 \cosh \beta h)$ are the probabilities for the central spin to be up $(+)$ or down $(-)$ in the field of its neighbors h.

We also note from Eq. (36) that the symmetric part of $\tilde{P}(t)$ is given

$$\tfrac{1}{2}[\tilde{P}^{z+1}(t) + \tilde{P}^{z+1}(-t)] = \int d\omega \left[\delta[\omega - 2(t+1)] \left[\frac{P(\omega/2) + P(-\omega/2)}{1 + e^{-\beta\omega}} \right] + \delta[\omega - 2(t-1)] \left[\frac{P(\omega/2) + P(-\omega/2)}{1 + e^{-\beta\omega}} \right] \right] = \int d\omega \, S(\vec{k}, \omega) \{ \delta[\omega - 2(t+1)] + \delta[\omega - 2(t-1)] \} \tag{39}$$

using the result in Eq. (29) of paper I. This relationship is interesting as all explicit thermal factors are now removed.

In Fig. 7 we compare the scaled distributions for $P(h)$ and $P^{z+1}(S)$ with the $P_\infty(S)$ values obtained by Bruce[3] and Binder.[4] The field $h = JS$ and we take $J=1$ for convenience in Fig. 7. Clearly, these small-block functions already capture the qualitative spirit of the universal critical distribution although further work is needed to see more precisely the progression to large L (see also Ref. 4).

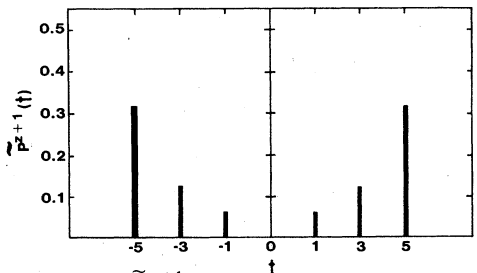

FIG. 6. $\tilde{P}^{z+1}(t)$ for the square net at T_c.

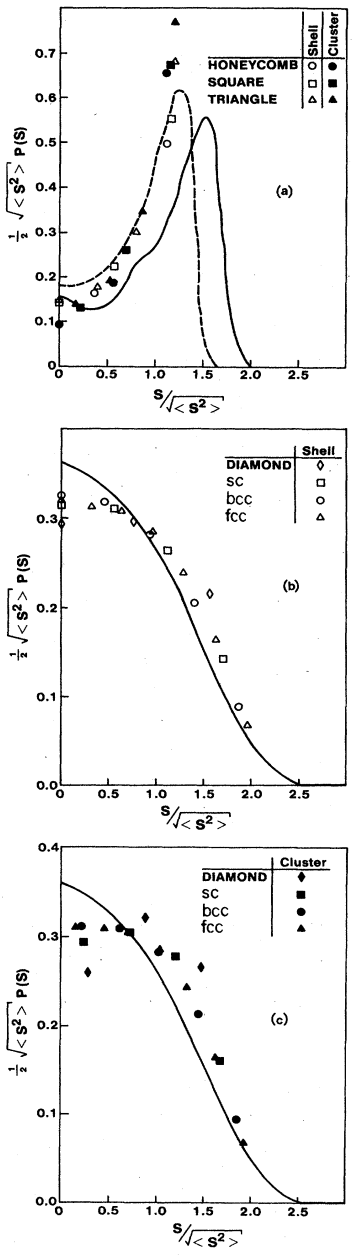

FIG. 7. (a) Comparison of $P(h)$ (shell), $P^{z+1}(S)$ (cluster), and $P_\infty(S)$ for 2D lattices. The dashed line is from Monte Carlo determination (Ref. 4) of $P_\infty(S)$ and the solid line is a renormalization-group (Ref. 3) estimate of $P_\infty(S)$. (b) Comparison of $P(h)$ (shell) and $P_\infty(S)$ for 3D lattices. The solid curve is the result of a Monte Carlo determination (Ref. 4) of $P_\infty(S)$ and of a virtually indistinguishable renormalization-group (Ref. 3) estimate. (c) Same as (b) but using $P^{z+1}(S)$ (cluster). All distributions have been normalized by the second moment so as to fit on the same scale. The field $h=JS$ and we take $J=1$ for convenience.

III. DISORDER POINTS IN ONE DIMENSION

There is currently much interest in systems with frustration[22] and competing interactions or fields, both in pure and in spatially random systems. Examples of pure systems are Ising antiferromagnets with topological frustration on nonbipartite lattices (such as the triangular net[5,23] and the face-centered-cubic lattice[24]) and anisotropic next-nearest-neighbor Ising (ANNNI) models.[25] Examples of disordered systems are the spin glasses and magnets in random fields. They are normally characterized by the existence of large ground-state degeneracies and hence residual entropies.[26] Disordered systems are the subject of paper III and the general pure frustrated case will not be discussed here. However, we do provide a discussion of two simple examples which provide a direct counting of ground-state degeneracies without elaborate techniques. These examples are both one dimensional, although higher-dimensional analogs with the same basic mechanism exist, but are such that lattice constraints complicate the counting problem, permitting exact solution only for specific 2D lattices.[7]

The examples we consider here are the antiferromagnetic (AF) chain in an external field and the next-nearest-neighbor chain with competing interactions. The standard thermodynamic properties and spin correlations have been studied by previous authors,[16] using transfer matrix techniques, and provide sufficient information to construct $P(h)$ directly. However, since we are concerned mainly with ground-state degeneracies and their effect on $P(h)$ it is interesting to construct explicitly the ground states.

Consider a one-dimensional Ising chain with nearest-neighbor antiferromagnetic interactions in the presence of an external field, with Hamiltonian

$$\mathcal{H}=J_0\sum_{i=1}^{N-1}\sigma_i\sigma_{i+1}-H\sum_{i=1}^{N}\sigma_i\ . \tag{40}$$

One can easily see that the lowest energy configuration is ferromagnetic for $|H|>2J_0$ while for $|H|<2J_0$ it is antiferromagnetic. However, when $|H|=2J_0$ the ground state is highly degenerate and any configuration is a ground state provided that no two adjacent spins point antiparallel to the field.

This ground-state degeneracy is conveniently enumerated with the help of the tree diagram of Fig. 8. Each level

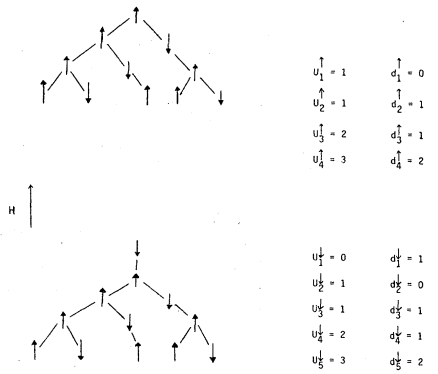

FIG. 8. "Tree" diagrams for counting the ground states of the 1D antiferromagnet in a field at its disorder point. Tracing a path from a top spin to any one of the corresponding bottom spins maps out a possible ground state.

on the tree represents a spin on the chain. Every path from the top to the bottom level maps out a ground state and hence the ground-state degeneracy of a system of N spins is equal to the number of branches at the Nth level.

There are two types of tree corresponding to the initial conditions $\sigma_1=\pm 1$. The rules for construction are that every down-spin must be followed by an up-spin while every up-spin branches into a down-spin and an up-spin. It is useful to count subsets of the set of all ground states based on the orientation of σ_1 and σ_N. We denote these subset numbers by

$$\begin{aligned} &u_N^{\uparrow}(\sigma_N=+1,\sigma_1=+1),\quad u_N^{\downarrow}(\sigma_N=+1,\sigma_1=-1)\ , \\ &d_N^{\uparrow}(\sigma_N=-1,\sigma_1=+1),\quad d_N^{\downarrow}(\sigma_N=-1,\sigma_1=-1)\ , \\ &u_N^{\downarrow}=u_{N-1}^{\uparrow}\ , \\ &d_N^{\downarrow}=d_{N-1}^{\uparrow}\ , \\ &d_N^{\uparrow}=u_{N-1}^{\uparrow}\ , \\ &u_N^{\uparrow}=u_{N-1}^{\uparrow}+d_{N-1}^{\uparrow}\ . \end{aligned} \tag{41}$$

Hence, the number of ground states at the Nth level, G_N, satisfies the relations

$$G_{N+1}=2u_N^{\uparrow}+d_N^{\uparrow} \tag{42}$$

and

$$G_{N+1}=G_N+G_{N-1}\ . \tag{43}$$

Equation (43) is the famous Fibonacci sequence. Denoting

$$\lim_{N\to\infty}\frac{G_{N+1}}{G_N}=\alpha \tag{44}$$

we have [from (43)]

$$\alpha=1+\alpha^{-1}\ , \tag{45}$$

whose only positive root is the golden ratio:

$$\alpha=(1+\sqrt{5})/2\ , \tag{46}$$

yielding the thermodynamic limit entropy per spin:

$$S=\lim_{N\to\infty}[k_B(\ln G_N)/N] \tag{47}$$

$$=k_B\ln[(1+\sqrt{5})/2]\simeq 0.4812k_B\ . \tag{48}$$

It is useful to note that

$$\lim_{N\to\infty}\left[\frac{u_N^{\uparrow}+d_N^{\uparrow}}{u_N^{\downarrow}+d_N^{\downarrow}}\right]=\alpha \tag{49}$$

which means that an up-spin generates a factor of α more ground-state configurations than does a down-spin. For a typical spin near the center of a large open chain we can build trees on either side so that

$$\frac{\text{Prob}(\sigma_i=+1)}{\text{Prob}(\sigma_i=-1)}=\alpha^2 \tag{50}$$

and hence, in the thermodynamic limit the magnetization per spin is

TABLE III. Possible ground-state configurations, the local field at the central site h/J_0, and the probability of occurrence of clusters of three spins in the AF Ising chain at the disorder point [model defined by Eq. (40)]. The parameter $\alpha=(1+\sqrt{5})/2$.

Configuration	h/J_0	Relative probabilities
↑↑↓	2	α
↑↑↑	0	α^2
↓↑↓	4	1
↑↓↑	0	α^2
↓↑↑	2	α

$$m=\frac{\alpha^2-1}{\alpha^2+1}=\frac{1}{\sqrt{5}}\simeq 0.4472\ , \tag{51}$$

a result which can also be obtained from the free energy.

In 1D, knowledge of the energy per bond and the magnetization immediately yields $P(h)$.[1] However, it may also be calculated usefully from these state counting arguments. In particular, consider clusters of three spins and the corresponding local field on the central site. The five possible clusters (three are ruled out as having two or more adjacent down-spins) are shown in Table III together with their probability weights [determined by analogy with Eq. (50)]. $P(h)$ is now easily written down as

$$P(h)=\sum_s w_s\delta(h-J_0 s)\ , \tag{52}$$

with

$$\begin{aligned} &w_0=2\alpha^2/(2\alpha^2+2\alpha+1)=1-1/\sqrt{5}\simeq 0.5528\ , \\ &w_{2J_0}=2\alpha/(2\alpha^2+2\alpha+1)=(3/\sqrt{5})-1\simeq 0.3416\ , \\ &w_{4J_0}=(2\alpha^2+2\alpha+1)^{-1}=1-2/\sqrt{5}\simeq 0.1056\ . \end{aligned} \tag{53}$$

These results are shown in Fig. 9 along with those on either side of the disorder point. The peak at $h=0$ clearly indicates that a finite fraction of the spins are free to flip at no cost in energy.

Another system, thermodynamically related to that of Eq. (40), is the 1D Ising chain in zero field with competing next-nearest-neighbor interactions with Hamiltonian

$$\mathcal{H}=-J_1\sum_i\sigma_i\sigma_{i+1}-J_2\sum_i\sigma_i\sigma_{i+2}\ . \tag{54}$$

Since there are no closed loops it is useful to define a new Ising variable,[17]

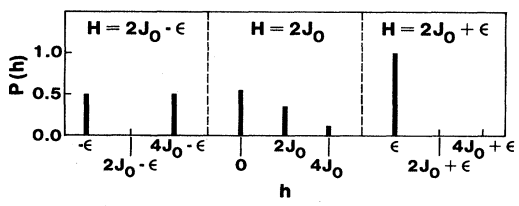

FIG. 9. $P(h)$ near the disorder point of a 1D Ising antiferromagnet at zero temperature in a field [see Eq. (40)]. Here, ϵ is an infinitely small positive quantity.

$$\tau_i=\sigma_i\sigma_{i+1},\quad \tau_i=\pm 1 \tag{55}$$

so that Eq. (54) transforms to

$$\mathscr{H}=-J_1\sum_i \tau_i - J_2\sum_i \tau_i\tau_{i+1}\,, \tag{56}$$

identical with Eq. (40). Consequently both models yield the same free energy; however, they have very *different* internal-field distributions. We shall consider again only the zero-temperature situations. Finite temperatures can be studied using the formalism of paper I and the knowledge of multispin correlations of the 1D AF chain in a field.[27,28] However, as in the previous model, there is no phase transition at finite temperature and the most significant physics from our present viewpoint arise from the high ground-state degeneracy at the disorder point $J_2=-J_1/2$, where $J_1>0$, $J_2<0$. Hence, we concentrate on $T=0$ near this point. From the equivalence of Eqs. (56) and (40) we easily deduce that if $J_2>-J_1/2$ the ground state is ferromagnetic while if $J_2<-J_1/2$ it consists of spins alternating in *pairs;* two up-spins, two down-spins, etc. At the disorder point $J_2=-J_1/2$, any spin configuration is a ground state provided no spin has two neighbors antiparallel to itself.

Define a paired bond to mean that two nearest neighbors are parallel. An unpaired bond consists of two antiparallel nearest neighbors. All the ground states can be constructed by requiring that every unpaired bond be followed by a paired bond while allowing a paired bond to be followed by either a paired or an unpaired bond. It is easy to see that these *bond* rules map into the *spin* rules of the previous problem and we can then write down essentially the same trees and recursion relations. This gives the same entropy for this disorder point as for the antiferromagnet in a field, which is required since their free energies are identical.

To determine $P(h)$, we must look at a cluster of five spins since each spin has four interacting neighbors. Table IV shows the possible ground-state configurations of five spin clusters along with the field at the central site and the relative probability for that configuration to occur. The latter is determined analogously to those given in Table III where now a factor of α is associated with a paired bond at the end of a cluster while an unpaired bond takes a factor of 1.

From Table IV, it is seen that $P(h)$ has the form of Eq. (52) but with J_0 replaced by J_1. There are seven delta functions with weights:

$$\begin{aligned}
w_0&=4\alpha^2/(6\alpha^2+8\alpha+2)=(3/\sqrt{5})-1\simeq 0.3416\,,\\
w_{\pm J_1}&=(\alpha^2+2\alpha)/(6\alpha^2+8\alpha+2)=(3-\sqrt{5})/4\simeq 0.1910\,,\\
w_{\pm 2J_1}&=2\alpha/(6\alpha^2+8\alpha+2)=1-2/\sqrt{5}\simeq 0.1056\,,\\
w_{\pm 3J_1}&=(6\alpha^2+8\alpha+2)^{-1}=7/4\sqrt{5}-\tfrac{3}{4}\simeq 0.0326\,.
\end{aligned} \tag{57}$$

In Fig. 10 we show $P(h)$ at the disorder point as well as on either side of the disorder point. Unlike the Hamiltonian (40), there is no field to break the symmetry in this problem and $P(h)$ is symmetric. It is interesting to note that as $P(h)$ approaches this disorder point from either side, it has the same limiting form, but that limit is different from the value precisely at the disorder point. Once again, the peak at $h=0$ gives an indication of the large number of spins that can be flipped at no cost in energy and hence of the finite entropy at $T=0$.

TABLE IV. Possible ground-state configurations, the local field at the central site h/J_1, and the probability of occurrence of clusters of five spins in the Ising chain with competing interactions at the disorder point [model defined by Eq. (54)]. The parameter $\alpha=(1+\sqrt{5})/2$.

Configuration	h/J_1	Relative probabilities
↑↑↑↑↑	1	α^2
↑↑↑↑↓	2	α
↓↑↑↑↑	2	α
↑↑↑↓↓	0	α^2
↓↓↑↑↑	0	α^2
↓↑↑↑↓	3	1
↓↓↑↑↓	1	α
↓↑↑↓↓	1	α
↑↑↓↑↓	−1	α
↑↓↓↑↑	−1	α
↑↑↓↓↓	0	α^2
↑↓↓↓↑	−3	1
↓↓↓↑↑	0	α^2
↓↓↓↓↑	−2	α
↑↓↓↓↓	−2	α
↓↓↓↓↓	−1	α^2

Finally we note some similarity between this distribution and that of the triangular antiferromagnet at the disorder point.[5] This suggests that the underlying physical mechanism for the infinite ground-state degeneracies are the same in both cases even though the mathematical treatment is more complicated in the triangular antiferromagnet. The ground-state entropy per spin for the triangular antiferromagnet is[23,29]

$$\frac{S}{k_B}=\tfrac{1}{2}\ln 2-\frac{3}{\pi}L\left[\frac{\pi}{6}\right]=0.3231\,,$$

where $L(x)$ is Lobachevskiy's function.[29,30] Compare this with the entropy S for the one-dimensional models, Eq. (48).

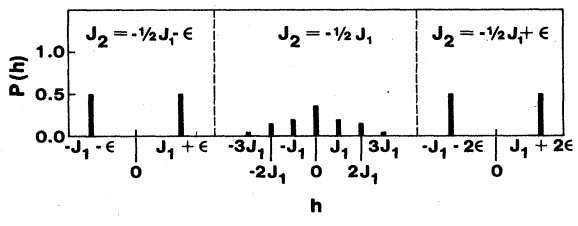

FIG. 10. $P(h)$ near the disorder point at zero temperature for an Ising chain with competing nearest- and next-nearest-neighbor interactions [see Eq. (54)]. Here, ϵ is an infinitely small positive quantity.

IV. CLASSICAL VECTOR SPINS

In this section we first establish a generalization of the concept of local fields for classical m-vector spins and obtain the formal analogs of the relations given in paper I connecting $P(\mathbf{h})$ with thermodynamic quantities. Numerous differences from Ising models will also be pointed out. Closed-form exact results are obtained only for the one-dimensional zero field and Bethe lattices, but these serve to illustrate the properties of $P(\mathbf{h})$ in the generalizations of paper I. Initially we shall consider general J_{ij} but explicit results will only be given for pure systems, leaving the study of random systems to paper III.

Consider the m-vector classical Heisenberg model in a field

$$\mathscr{H}=-\tfrac{1}{2}\sum_{i,j}J_{ij}\hat{\mathbf{S}}_i\cdot\hat{\mathbf{S}}_j-\sum_i\mathbf{H}_i\cdot\hat{\mathbf{S}}_i\ , \tag{58}$$

where the $\hat{\mathbf{S}}$'s are unit vectors on an m-dimensional sphere, and J_{ij} and $\mathbf{H}_i$ are arbitrary. Analogously to paper I we define the local field h_i as

$$\mathbf{h}_i=\sum_j J_{ij}\hat{\mathbf{S}}_j+\mathbf{H}_i\ . \tag{59}$$

The obvious generalization of Eq. (6) of paper I is

$$\langle\mathbf{O}\cdot\hat{\mathbf{S}}_i\rangle=\langle\mathbf{O}\cdot\hat{\mathbf{h}}_i\mathscr{L}_m(\beta h_i)\rangle\ , \tag{60}$$

where $\mathbf{O}$ is *any* classical operator not containing $\hat{\mathbf{S}}_i$, $h_i=|\mathbf{h}_i|$, $\hat{\mathbf{h}}_i=\mathbf{h}_i/|h_i|$, a unit vector, and the generalized Langevin function:

$$\mathscr{L}_m(x)=\frac{\partial}{\partial x}\ln[I_{m/2-1}(x)/x^{m/2-1}]$$

$$=[I_{m/2}(x)/I_{m/2-1}(x)]\ . \tag{61}$$

The $I_\nu(x)$ are modified Bessel functions of order ν.

Choosing $\mathbf{O}$ to be an arbitrary unit vector $\hat{\mathbf{u}}$, we obtain

$$\mathbf{m}_i\cdot\hat{\mathbf{u}}=\langle\hat{\mathbf{S}}_i\rangle\cdot\hat{\mathbf{u}}=\hat{\mathbf{u}}\cdot\langle\hat{\mathbf{h}}_i\mathscr{L}_m(\beta h_i)\rangle \tag{62}$$

and hence the local magnetization is

$$\mathbf{m}_i=\langle\hat{\mathbf{h}}_i\mathscr{L}_m(\beta h_i)\rangle\ . \tag{63}$$

Similarly, the choice of $\mathbf{O}$ as $\mathbf{h}_i$ yields

$$\langle\hat{\mathbf{S}}_i\cdot\mathbf{h}_i\rangle=\langle h_i\mathscr{L}_m(\beta h_i)\rangle\ . \tag{64}$$

These are the analogs of Eqs. (7) and (8) of paper I. The analog of Eq. (9) of paper I for the "local energy" E_i is

$$E_i=-\tfrac{1}{2}\langle(\mathbf{h}_i+\mathbf{H}_i)\cdot\hat{\mathbf{S}}_i\rangle$$

$$=-\tfrac{1}{2}\langle(h_i+\mathbf{H}_i\cdot\hat{\mathbf{h}}_i)\mathscr{L}_m(\beta h_i)\rangle\ . \tag{65}$$

The total magnetization M and total energy E are given by

$$\mathbf{M}=\sum_i\mathbf{m}_i\ , \tag{66}$$

$$E=\sum_i E_i\ . \tag{67}$$

The analog of Eq. (11) of paper I for the probability distribution of the local field at site i is

$$P_i(\mathbf{h})=\langle\delta(\mathbf{h}-\mathbf{h}_i)\rangle,\quad \mathbf{h}_i=\sum_j J_{ij}\hat{\mathbf{S}}_j+\mathbf{H}_i\ , \tag{68}$$

whence

$$\mathbf{m}_i=\int d\mathbf{h}\,\hat{\mathbf{h}}\mathscr{L}_m(\beta h)P_i(\mathbf{h})\ , \tag{69}$$

$$E_i=-\tfrac{1}{2}\int d\mathbf{h}(h+\mathbf{H}_i\cdot\hat{\mathbf{h}})\mathscr{L}_m(\beta h)P_i(\mathbf{h})\ , \tag{70}$$

where $d\mathbf{h}$ is an m-dimensional volume element. Similarly,

$$M=N\int d\mathbf{h}\,\hat{\mathbf{h}}\mathscr{L}_m(\beta h)P(\mathbf{h}) \tag{71}$$

and, specializing to a uniform external field H,

$$E=-\tfrac{1}{2}N\int d\mathbf{h}\,h\mathscr{L}_m(\beta h)P(\mathbf{h})-HM/2\ , \tag{72}$$

where

$$P(\mathbf{h})=N^{-1}\sum_i P_i(\mathbf{h})\ . \tag{73}$$

Note that in general P,M,E, etc., are temperature dependent but we do not indicate this explicitly.

Because of the nontrivial nature of the dynamics of vector spins we cannot express the neutron scattering response function $S(\vec{k},\omega)$ in terms of $P(\mathbf{h})$ alone.

Let us now consider setting up a formulation for obtaining $P(\mathbf{h})$, concentrating on the pure ferromagnetic nearest-neighbor case:

$$J_{ij}=\begin{cases}J=1 & (ij)\text{ nearest neighbors}\ ,\\ 0 & \text{otherwise}\ .\end{cases}$$

In the pure case

$$P(\mathbf{h})=N^{-1}\sum_i P_i(\mathbf{h})=\left\langle\delta\left[\mathbf{h}-\sum_{j=1}^{z}\hat{\mathbf{S}}_j\right]\right\rangle\ , \tag{74}$$

where the sum extends over nearest-neighbor spins. Then, in terms of the characteristic function $G(\mathbf{y})$,

$$P(\mathbf{h})=\frac{1}{(2\pi)^m}\int d\mathbf{y}\,e^{-i\mathbf{h}\cdot\mathbf{y}}G(\mathbf{y})\ , \tag{75}$$

where

$$G(\mathbf{y})=\left\langle\prod_{j=1}^{z}e^{i\mathbf{y}\cdot\hat{\mathbf{S}}_j}\right\rangle\ , \tag{76}$$

the product being taken over the z nearest neighbors of a spin $\hat{\mathbf{S}}_i$.

The formulation of paper I *cannot* be carried forward to obtain $G(\mathbf{y})$ in terms of a *finite* set of multispin correlations alone. This is because $e^{i\mathbf{y}\cdot\hat{\mathbf{S}}_j}$ cannot be decomposed into a finite-order polynomial in $\hat{\mathbf{S}}_j$, unlike the form

$$e^{iy\sigma_j}=\cos y+i\sigma_j\sin y$$

which holds only for $\sigma_j=\pm1$. Furthermore, $P(\mathbf{h})$ is now a *continuous* distribution and knowledge of a finite set of its moments is *not* sufficient to reconstruct the distribution, unlike the situation in the Ising case where the first $(z+1)$ moments suffice. Instead, a knowledge of *all* eigenvalues and eigenfunctions of the transfer integral

operator is necessary. With the exception of one dimension or the Bethe lattice this is completely lacking. In the latter cases the calculation is straightforward but tedious; for example, in one dimension:

$$G(\mathbf{y})=\sum_n(\lambda_n/\lambda_0)^2\left[\int d\hat{\mathbf{S}}\psi_0(\hat{\mathbf{S}})e^{i\mathbf{y}\cdot\hat{\mathbf{S}}}\psi_n^*(\hat{\mathbf{S}})\right]\times\left[\int d\hat{\mathbf{S}}\psi_0^*(\hat{\mathbf{S}})e^{i\mathbf{y}\cdot\hat{\mathbf{S}}}\psi_n(\hat{\mathbf{S}})\right], \tag{77}$$

where $\psi_n(\hat{\mathbf{S}})$ and λ_n are the eigenfunctions and eigenvalues of the transfer integral operator.[29] All the integrals can be evaluated using product expansions of $e^{i\mathbf{y}\cdot\hat{\mathbf{S}}}$, as well as using addition formulae[31] to sum the infinite series which results. The details are not too illuminating, so we shall not dwell on this approach here, although it represents the only systematic method for obtaining $P(\mathbf{h})$ from these eigenfunctions (if known) of which we are aware.

In one dimension or for the Bethe lattice we shall instead exploit the basic formula [Eq. (6)] to advantage. Here, the traces are integrals over m spheres and the terms simplify. Let us proceed directly with a Bethe lattice, the chain then being a special case with $z=2$. As discussed earlier we may express the Hamiltonian as

$$\mathscr{H}=-\sum_{j=1}^{z}\hat{\mathbf{S}}_0\cdot\hat{\mathbf{S}}_j-\mathbf{H}_0\cdot\hat{\mathbf{S}}_0-\mathbf{H}_1\cdot\sum_{j=1}^{z}\hat{\mathbf{S}}_j\ , \tag{78}$$

where $\mathbf{H}_0$ is the external field, eventually to be set to zero, and $\mathbf{H}_1$ is the internal self-consistent field. Then the partition function is

$$Z=\int\frac{d\hat{\mathbf{S}}_0}{\omega_p}\exp(\beta H_0\cos\theta_0)(Z')^z\ , \tag{79}$$

where

$$Z'=\int\frac{d\hat{\mathbf{S}}_i}{\omega_p}\exp(\beta\hat{\mathbf{S}}_0\cdot\hat{\mathbf{S}}_i+\beta H_1\cos\theta_i)$$

$$=\frac{1}{p}\sum_l(2l+p)\lambda_l(\beta)\lambda_l(\beta H_1)C_l^{p/2}(\cos\theta_0)\ . \tag{80}$$

Here, $C_l^{p/2}$ is a Gegenbauer polynomial, $p=m-2$,

$$\omega_p=2\pi^{1+p/2}/\Gamma(1+p/2)\ ,$$

the θ_i are polar angles measured relative to H_1, and

$$\lambda_l(x)=\frac{2^{p/2}\Gamma(1+p/2)I_{l+p/2}(x)}{x^{p/2}}\ . \tag{81}$$

Using standard properties of Bessel functions[31] we have

$$Z=\int\frac{d\hat{\mathbf{S}}_0}{\omega_p}e^{\beta H_0\cos\theta_0}\left[\frac{2^{p/2}\Gamma(1+p/2)I_{p/2}(\Phi)}{\Phi^{p/2}}\right]^z, \tag{82}$$

where

$$\Phi=\beta(1+2H_1\cos\theta_0+H_1^2)^{1/2}\ .$$

Self-consistency requires that

TABLE V. $P(\mathbf{h},T=\infty)$ for $m=3$ classical vector spins for $z=2,3,4$, where $h=|\mathbf{h}|$.

z	T_c	$P(\mathbf{h},T=\infty)$
2	0.0000	$\frac{1}{8\pi h}$, $0<h<2$
3	0.5566	$\frac{1}{8\pi}$, $0<h<1$
		$\frac{1}{16\pi h}(3-h)$, $1<h<3$
4	0.9307	$\frac{1}{64\pi h}(8h-3h^2)$, $0<h<2$
		$\frac{1}{64\pi h}(4-h)^2$, $2<h<4$

$$\left.\frac{\partial\ln Z}{\partial(\beta H_0)}\right|_{H_0=0}=\frac{1}{z}\left.\frac{\partial\ln Z}{\partial(\beta H_1)}\right|_{H_0=0}, \tag{83}$$

leading to the determining equation for H_1:

$$\int\frac{d\hat{\mathbf{S}}_0}{\omega_p}\left[\frac{I_{p/2}(\Phi)}{\Phi^{p/2}}\right]^z\left[\cos\theta_0-\frac{\beta(\cos\theta_0+H_1)}{\Phi}\mathscr{L}_m(\Phi)\right]=0\ , \tag{84}$$

where $\mathscr{L}_m(\Phi)$ is the Langevin function Eq. (61). Note that $H_1=0$ is always a solution and indeed is the only solution for $T>T_c$, where T_c is readily obtained from a power-series expansion in H_1 yielding

$$\mathscr{L}_m(\beta_c)=1/(z-1),\quad \beta_c=1/k_BT_c\ . \tag{85}$$

For $T>T_c$, $H_1=0$, Eq. (82) also simplifies:

$$Z=[2^{p/2}\Gamma(1+p/2)]^{z+1}\frac{I_{p/2}(\beta H_0)}{(\beta H_0)^{p/2}}\left[\frac{I_{p/2}(\beta)}{\beta^{p/2}}\right]^z. \tag{86}$$

In general the solution of Eq. (84) is a numerical problem. Of the three terms defining $P(\mathbf{h})$ which we rewrite as

$$P(\mathbf{h})=Z_1(\beta h)\langle\delta(\mathbf{h}-\mathbf{h}_i)\rangle'\frac{\mathrm{Tr}'(e^{-\beta\mathscr{H}'})}{\mathrm{Tr}(e^{-\beta\mathscr{H}})}\ , \tag{87}$$

the first term is the most straightforward and yields

$$Z_1(\beta h)=\gamma_pI_{p/2}(\beta h)/(\beta h)^{p/2}\ , \tag{88}$$

where

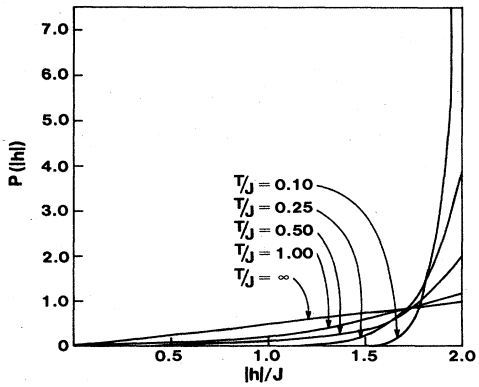

FIG. 11. $P(|\mathbf{h}|)=4\pi h^2P(\mathbf{h})$ for $m=3$ spins on a chain.

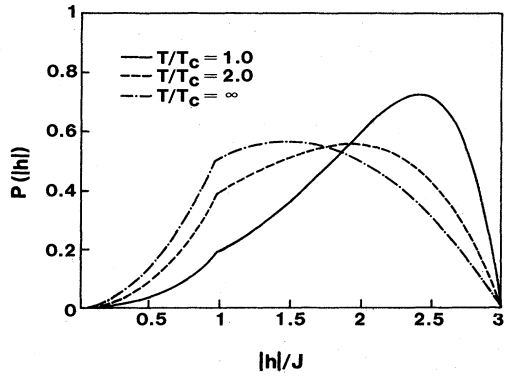

FIG. 12. $P(|\mathbf{h}|)=4\pi h^2 P(\mathbf{h})$ for $m=3$ spins on a Bethe lattice of coordination $z=3$. The first and higher derivatives of $P(|\mathbf{h}|)$ are discontinuous at $|\mathbf{h}|=J$ at all temperatures.

$$\gamma_p = 2^{p/2}\Gamma(1+p/2)\ . \tag{89}$$

The last term corresponds to z disconnected Bethe lattices *correlated* by the field $\mathbf{H}_1$:

$$\frac{\mathrm{Tr}'(e^{-\beta\mathscr{H}'})}{\mathrm{Tr}(e^{-\beta\mathscr{H}})} = \frac{[I_{p/2}(\beta H_1)/(\beta H_1)^{p/2}]^z}{\int \frac{d\hat{\mathbf{S}}_0}{\omega_p}[I_{p/2}(\Phi)/\Phi^{p/2}]^z}\ . \tag{90}$$

Above T_c the middle term is essentially the classic problem of random walks, solved by Rayleigh[32] for three-dimensional lattices (corresponding to $m=3$ here) for z up to 6. For general $m\neq 3$, the problem is analytically intractable except for some special cases; $m=2$ and $z=2$ and 3, which involve elliptic integrals, $z=3$, and $m>3$, which involve hypergeometric functions[31] and the trivial case of $z\to\infty$.[33] For $T<T_c$ only numerical solution appears possible. A final formula for $P(\mathbf{h})$ for all T is

$$P(\mathbf{h}) = \frac{\gamma_p \frac{I_{p/2}(\beta h)}{(\beta h)^{p/2}} \int \frac{d\mathbf{r}}{(2\pi)^{p+2}} e^{-i\mathbf{h}\cdot\mathbf{r}} \left[\frac{I_{p/2}(\Phi')}{(\Phi')^{p/2}}\right]^z}{\int \frac{d\hat{\mathbf{S}}_0}{\omega_p}\left[\frac{I_{p/2}(\Phi)}{\Phi^{p/2}}\right]^z}\ , \tag{91}$$

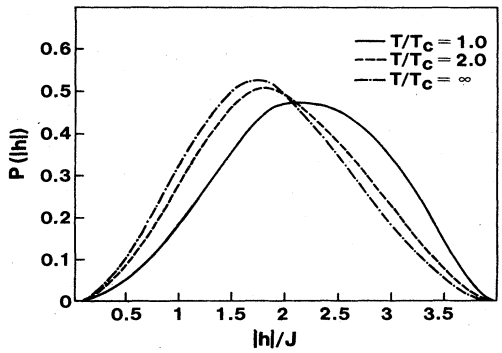

FIG. 13. $P(|\mathbf{h}|)=4\pi h^2 P(\mathbf{h})$ for $m=3$ spins on a Bethe lattice with $z=4$. The second and higher derivatives of $P(|\mathbf{h}|)$ are discontinuous at $|\mathbf{h}|=2J$ at all temperatures.

where

$$\Phi' = (\beta^2 H_1^2 + 2\beta H_1 i r\theta_r - r^2)^{1/2} \tag{92}$$

with $\mathbf{H}_1$ being the polar axis and θ_r the polar angle of $\mathbf{r}$ with modulus $r=|\mathbf{r}|$. $H_1=|\mathbf{H}_1|$ is obtained from Eq. (84). For finite $H_1(T<T_c)$, the case of spontaneous magnetization, we see that $P(\mathbf{h})$ acquires an angular dependence through the integrands which are no longer spherically symmetric. For Heisenberg spins ($m=3$) and $T\geq T_c$ Eq. (91) simplifies to

$$P(\mathbf{h}) = P(\mathbf{h}, T=\infty)\left[\frac{\sinh(\beta h)/\beta h}{(\sinh\beta/\beta)^z}\right], \tag{93}$$

where $P(\mathbf{h}, T=\infty)$ is given in Table V. In Figs. 11–13 we exhibit $P(|\mathbf{h}|)=4\pi h^2 P(\mathbf{h})$ for $z=2,3,4$. The peaks in $P(|\mathbf{h}|)$ are progressively shifted to larger h as $T\to T_c$. Van Hove–type singularities are noticeable for $z=3$ in Fig. 12. These singularities weaken as z increases until eventually $P(\mathbf{h})=\delta(\mathbf{h}-\mathbf{H}_1)$ in the mean-field limit, easily shown as in the Ising case. Finally, for completeness, we give the result for the general m-vector chains:

$$P(\mathbf{h}) = \left[\frac{\beta}{2h}\right]^{p/2} \frac{1}{\pi^{1/2}\omega_p \Gamma[(p+1)/2]} \times \left[\frac{1}{h}\right]\left[1-\frac{h^2}{4}\right]^{(p-1)/2} \frac{I_{p/2}(\beta h)}{I_{p/2}^2(\beta)}\ , \tag{94}$$

$$m = p+2,\quad 0<h<2\ .$$

Recovering the energy:

$$E/N = -\mathscr{L}_m(\beta)$$

is a short exercise requiring the properties of Bessel functions.[29,31]

V. CONCLUSIONS

We have shown that the local magnetic field distribution for Ising models exhibits a quasiuniversal shape determined principally by dimension rather than coordination. Near the critical temperature these shapes are closely analogous to those of the universal block-spin distribution function for blocks of dimension large compared with the lattice spacing but small compared with the correlation length. Both functions provide useful thermodynamic information, that from the local-field distribution as a function of temperature being complete (for pure systems in uniform fields). Presumably a similar (quasi) universality exists for higher-dimensional classical spins, and certainly $P(\mathbf{h},T)$ provides the corresponding thermodynamic quantities, but we have only examined explicitly systems on Bethe lattices.

We have also demonstrated for some one-dimensional systems with $T=0$ disorder points that not only is there a degeneracy singularity associated with these points but also a discontinuity of shape of $P(h)$. It would be of interest to study systems with analogous frustration in higher space and spin dimensions.

ACKNOWLEDGMENTS

We would like to thank Dr. P. Beale for drawing our attention to the universal block-spin distribution function and the National Science Foundation (U.S.) and Science and Engineering Research Council (United Kingdom) for financial support. We would also like to thank Ms. W. Tang for obtaining the results for the second-neighbor Ising chain presented in Sec. III. One of us (M.T.) would like to thank Exxon for financial support.

---

*Present address: Department of Materials Science, University of Southern California, Los Angeles, CA 90089.

[1]M. Thomsen, M. F. Thorpe, T. C. Choy, and D. Sherrington, Phys. Rev. B **30**, 250 (1984), hereafter referred to as paper I. We will establish notations consistent with this paper.

[2]M. Thomsen, M. F. Thorpe, T. C. Choy, D. Sherrington, and H. J. Sommers (unpublished), hereafter referred to as paper III.

[3]A. D. Bruce, J. Phys. C **14**, 3667 (1981).

[4]K. Binder, Z. Phys. B **43**, 119 (1981).

[5]T. C. Choy and D. Sherrington, J. Phys. A **16**, L265 (1983); **16**, 3691 (1983).

[6]T. C. Choy, J. Math. Phys. **25**, 3558 (1984).

[7]T. C. Choy (unpublished).

[8]Some of the results in this section are contained in M. Thomsen, Ph.D. thesis, Michigan State University, 1984, to which reference can be made for further details.

[9]B. Frank, C. Y. Cheung, and O. G. Mouritsen, J. Phys. C **14**, 1233 (1982).

[10]C. Domb, in *Phase Transitions and Critical Phenomena,* edited by C. Domb and M. S. Green (Academic, New York, 1974), Vol. 3.

[11]D. S. Gaunt, M. F. Sykes, and S. McKenzie, J. Phys. A **12**, 871 (1979).

[12]N. Metropolis, A. W. Rosenbluth, M. N. Rosenbluth, A. H. Teller, and E. Teller, J. Chem. Phys. **21**, 1087 (1953).

[13]T. P. Eggarter, Phys. Rev. B **9**, 2989 (1974).

[14]H. A. Bethe, Proc. R. Soc. London, Ser. A **150**, 552 (1935).

[15]R. E. Peierls, Proc. Cambridge Philos. Soc. **32**, 477 (1936).

[16]C. Domb, Adv. Phys. **9**, 251 (1960).

[17]M. F. Thorpe, in *Excitations in Disordered Systems,* Vol. B78 of *Nato Advanced Study Institute Series,* edited by M. F. Thorpe (Plenum, New York, 1982).

[18]For example, compare Eqs. (29)—(31) with Eq. (20).

[19]We have thus made precise here the terms local field and mean field. The two can only be used interchangeably when $z \to \infty$.

[20]M. Cassandro and G. Jona-Lasinio, Adv. Phys. **27**, 913 (1979).

[21]We label the center spin as S_0 and its surrounding neighbors cyclically from S_1 to S_z as in paper I.

[22]G. Toulouse, Commun. Phys. **2**, 115 (1977).

[23]G. H. Wannier, Phys. Rev. **79**, 357 (1950); Phys. Rev. B **7**, 5017 (1973).

[24]A. Danielian, Phys. Rev. Lett. **6**, 670 (1961).

[25]See, e.g., P. Bak, Rep. Prog. Phys. **45**, 587 (1982).

[26]The fact that this violates the third law of thermodynamics imposes a limit at low temperatures on the validity of an Ising description for any real system. Therefore, any such studies without quantum mechanics must be taken as necessarily incomplete.

[27]J. F. Dobson, J. Math. Phys. **10**, 40 (1969).

[28]J. Stephenson, Can. J. Phys. **48**, 1724 (1970).

[29]T. C. Choy (unpublished).

[30]I. S. Gradshteyn and I. M. Ryzhik, *Table of Integrals, Series and Products* (Academic, New York, 1980).

[31]G. N. Watson, *A Treatise on the Theory of Bessel Functions* (Cambridge University, Cambridge, 1966).

[32]S. Chadrasekhar, Rev. Mod. Phys. **15**, (1943); Lord Rayleigh, Philos. Mag. **6**, 37 (1919).

[33]The case of $z \to \infty$ is again trivial of course, because of the central limit theorem.